Available online at www.CivileJournal.org

Civil Engineering Journal

(E-ISSN: 2476-3055; ISSN: 2676-6957)

Vol. 9, No. 04, April, 2023

Control Parameters for the Long-Term Tensile and Compressive Strength of Stabilized Sedimentary Silt

Wagner Teixeira [1], Jair Arrieta Baldovino [2*], Ronaldo Izzo [1]

[1] Department of Civil Construction, Federal University of Technology-Parana, Campus Curitiba, Curitiba, 81280-340, Brazil.

[2] Department of Civil Engineering, Universidad de Cartagena, Cartagena de Indias, 130015, Colombia.

Received 13 January 2023; Revised 07 March 2023; Accepted 21 March 2023; Published 01 April 2023

Abstract

The yellow-layer soils of the Guabirotuba formation in Brazil are problematic due to their expansive nature and low-bearing capacity. There has been little exploration into stabilizing these soils using a calcium-based binder. In addition, existing methods for dosing lime to fine and coarse-grained soils using the porosity-to-lime index (η/L_{iv}) have primarily focused on non-optimal compaction conditions to determine the split tensile and compressive strengths and empirical relationships between both tests while ignoring the study of optimal lime-soil mixes compaction conditions. Therefore, the objective of this research is to examine the unconfined compressive (q_u) and split tensile (q_t) behavior of a traditional Guabirotuba yellow silt stabilized with dolomitic hydrated lime (L) under standard, intermediate, and modified effort conditions and the correlation between q_u and q_t. The lime-soil blends were cured for up to 180 days, and 3-9% lime percentages were used under optimum compaction conditions (maximum dry density and optimum water content). The porosity/lime index (η/L_{iv}), a semi-empirical index, was utilized to investigate the evolution of q_u and q_t over the short and long term. η/L_{iv}varied between 6-25% by volume. Furthermore, the q_t/q_u index was calculated to be between 0.12-0.20, depending on the curing time, independent of lime addition and compaction effort used. Equations well-suited to a power function dosing q_t and q_u based on curing time and η/L_{iv} index was proposed. Finally, some dosages of soil-lime mixtures were proposed for possible applications in geotechnical engineering, applying the porosity and volumetric binder index in optimal compaction conditions, which had not been applied before for lime-improved soils.

Keywords: Porosity/Lime Ratio; Unconfined Compressive; Splitting Tensile Strength; Guabirotuba Soils.

1. Introduction

The use of lime as an additive in soil treatment is the oldest known chemical stabilization method, used in the most varied applications, such as the Appian Way, built by the Romans. Soil-lime can be defined as the product resulting from the intimately compacted mixture of soil (generally clay), lime, and water, in proportions established through dosage. The addition of lime to the soil has been denominated in different ways, according to the author, and terms such as stabilized soil, improved soil, modified soil, and treated soil are commonly used. In general, the criterion for adopting one or another denomination is the degree of change in the properties of the natural soil as a function of the amount of binder applied [1–4]. However, the processes are conceptually the same: the introduction and mixing of lime into the soil to obtain properties such as strength or deformability suitable for a given engineering use.

Soil-lime is used when there is no material or combination of materials with resistance, deformability, and permeability characteristics suitable for the project. Lime stabilization is commonly used in road construction and is

* Corresponding author: jarrietab2@unicartagena.edu.co

http://dx.doi.org/10.28991/CEJ-2023-09-04-03

generally used as a base or sub-base for pavements. The soil improvement technique can also be used for small building foundations, soils with low bearing capacity, or volumetric stability. Such conditions are problematic because they can cause severe pathologies in the building. The solution traditionally used to support loads of buildings in these places is deep foundations. These cross the less resistant material and are laid in deeper layers with greater support capacity [5–8]. However, this technical solution may make it unfeasible, for example, for works on low-cost housing developments, where investment in foundations may become a large portion of the project's total value. Many methods of evaluating the durability of lime-stabilized materials have been studied. Among these, we can highlight weight loss by abrasion, water absorption, pulse propagation velocity, volume variation, and resistance measurements. The most common laboratory methods are loss-in-weight and loss-in-strength for specimens subjected to wet-dry or freeze-to-thawing cycles [9, 10]. Thus, the resistance of soil-lime mixtures to weathering is influenced by the content and type of lime, the curing time, the compaction energy, and the type of soil. Lime content is so critical that a minimum of 5% is recommended, even though lower levels can produce specified strengths. Durability also increases with curing time and compaction energy. The primary consideration regarding the durability of soil-lime mixtures is resistance to freeze-thaw cycles. Prolonged periods of exposure to water produce a little harmful effect.

Studies carried out in recent years in southern Brazil (e.g., [2, 11–13]) have shown that using foundations supported on double-layer systems, the upper one consisting of compacted cemented soils, is an alternative technique that can be used in cases where there are layers of low-grade soils, strength, and load level of buildings are low. In addition, the permeability of lime-stabilized soils can be modified by methods such as compaction or injection. In clayey materials, the use of flocculants (for example, polyphosphates) can reduce the permeability significantly, but the use of flocculants lime hydroxide-$Ca(OH)_2$ or (gypsum) increases the permeability value. At present, some substances introduced into the soil in the form of an emulsion can significantly reduce its permeability (these substances can exert unfavourable effects on the soil's resistance to shear stress). Another critical application of soil-lime has been in the protection of slopes against erosion in hydraulic works, for example, in the Friant-Kern irrigation canal in California, where pulverized pure lime (3-5%) was used [14]. Both in terms of tightness and stability, the channel, with a flow of 150 m^3/min, did not show any significant erosion after one year of continuous service. Most artificial structures involve the use of compacted soil. The compaction process produces a degree of saturation generally in the range of 75 to 90% in the soil. Dams, embankments, roads, and embankments are typical earth structures from compacted soils [15].

The chemical stabilization usually applied in road paving works uses lime, cement, phosphorus compounds, petroleum derivatives (asphalt, tar, bitumen, asphalt, and emulsions), chlorides, resins, slag, polymers, waste or recyclable materials (industrial, domestic, or urban), industrial by-products, chemical reagents and sometimes combinations of these. Chemical stabilization by cement and lime is a proven technique for improving soil performance. It has been in constant development since its introduction in the middle of the last century, one of the most notable changes over the years being the requirement to use exclusively land located directly on a project's land reserve to build infrastructure [13, 15, 16].

Lime also has excellent application in the stabilization of soft soils and expansive soils. Among the design positions available in geotechnical engineering in extraordinarily soft and expansive soils, the authors highlight the following: avoidance, displacement, replacement, conventional landfills, overload, geosynthetic reinforcements, vertical drains, geotubes, surface layer treatment by mixing with a dry binder, columns of soil mixed with binders, columns of granular material, embankments reinforced with geosynthetics supported on columns (granular material or mixture of soil with binder) or piles, backfill on staked concrete slab and freezing. Adopting one or more technical solutions is mainly associated with the type of work and the thickness of the low resistance layer [17].

Lime-stabilized soils are normally field-compacted at the optimum moisture to obtain the maximum dry bulk density as determined in the Proctor compaction test. However, studies with soil-lime and soil-cement show that in some cases, the moisture content that provides maximum strength and durability is not necessarily equal to the moisture content that generates the highest apparent dry mass but a slightly lower value to the optimal content [18]. According to Metcalf et al. [19], the unconfined compressive strength generally increases linearly with the amount of lime up to a certain level, usually 8% for clayey soils. From this point on, the strength increase rate decreases with the amount of lime because soil-lime mixtures present a slow cementation that will depend on the soil type. Besides, no optimum lime content produces maximum strength in stabilized soil. They pointed out the content and type of lime, the type of soil, the specific weight, and the time and type of curing as the main factors influencing the resistance of soil and lime mixtures. In soils rich in kaolinite, adding calcium lime promotes more excellent resistance than dolomite, with the compressive strength being a simple linear function of the added lime content. The relationship is a quadratic equation for soils containing montmorillonite, and the best effects are obtained by adding dolomitic lime [20].

Although there are various studies about the variables that influence the strength of stabilized soils with lime, the impact of the porosity/binder relationship has not yet been studied when the silt-lime mixtures are compacted on optimal conditions of the Proctor effort. Therefore, this investigation addresses that gap in the literature. This research, by identifying and quantifying the essential variables in the control of the behavior of silt soil artificially treated with lime, aims to obtain subsidies so that, from the refined manipulation of such variables through dosage, it can be achieved objectively and with more excellent reliability the required properties in terms of compaction, unconfined compressive strength, and splitting tensile strength. In addition, it aims to obtain a comparison of the impacts of the porosity/lime ratio on the mechanical strength of the soil stabilized with lime. For this, lime percentages from 3 to 9% and curing times of up to 180 days are added. In addition, standard, intermediate, and modified compaction energies will be implemented.

2. Experimental Programme

There were three distinct phases to the experimental program. First, the particle size distribution and specific gravity of soil and lime were determined according to ASTM D2487 [21], ASTM 4318 [22], and ASTM D854 [23]. Based on the modified Initial Consumption of Lime (ICL), the minimum quantity of lime required for stabilization was calculated [24]. As described in the following section, the final phase consisted of molding, curing, and testing specimens subjected to unconfined compressive and split tensile tests. Figure 1 shows the experimental program of the lime-soil compacted blend characterization tests.

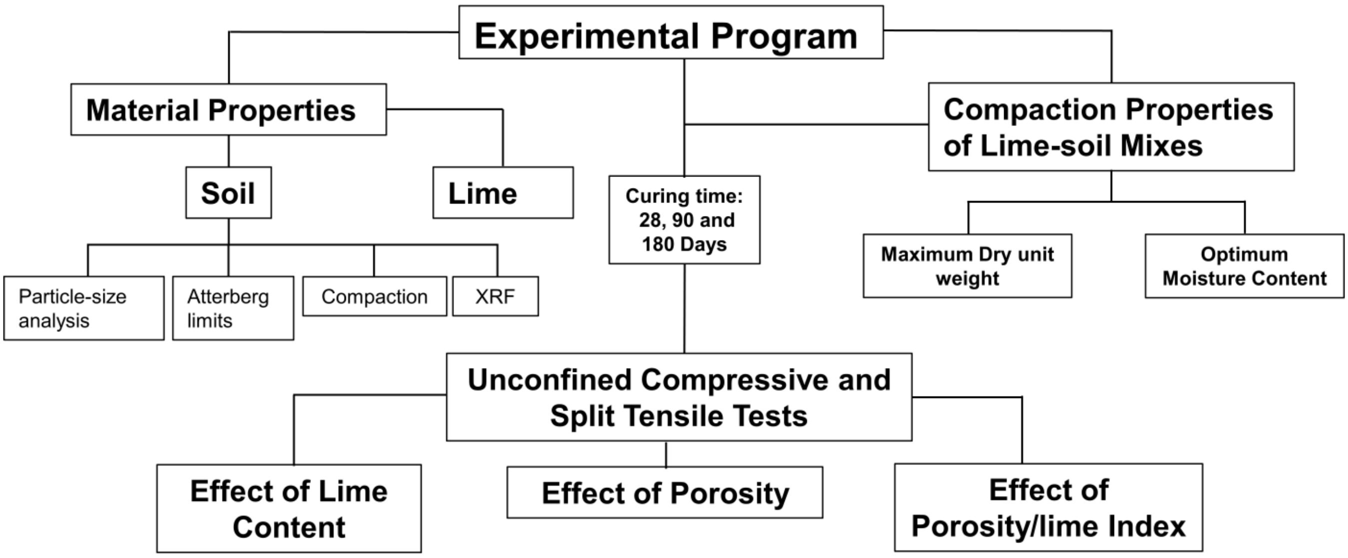

Figure 1. Experimental Program

2.1. Materials

Soil extraction (from the Guabirotuba Formation in Curitiba, Brazil) was carried out by manual excavation in the lower third of a slope cut with a slight slope adjacent to the internal road of the development, reaching approximately a depth of 0.50 meters since the site was already superficially cleaned. Therefore, in one of the cut slopes of the project's earthworks, around 200 kg of undisturbed samples were collected, which were later packed in plastic bags and transported to the laboratory. The granulometric distribution of the dispersive soil was calculated. Coarse sieving and conventional sedimentation tests were carried out, followed by fine sieving, according to NBR 7181 [25], using a deflocculant. In addition, laser analysis of the particles less than 0.15 mm was measured.

Figure 2 displays the particle size distribution curve of the soil sample. The soil is composed of almost 57% silt and 7% clay, in accordance with the Brazilian standard NBR 6502 and as presented in Table 1. Thus, the soil was classified as MH-sandy silt with high plasticity in agreement with international standard ASTM 2487 [21]. According to the Transportation Research Board (of AASHTO) classification, the soil can be classified as A-7-5 (i.e., for clays/silts: Plasticity Index ≤ Limit Liquid−30). As a result of the laser granulometry and sieve granulometry tests, the particle size distribution has been modified. Consistent with the MCT (Miniature, Compacted, Tropical) method, the soil is also classified as non-lateritic [26]. Another property of soil samples was characterized in Table 1. The soil in the field (slope) presents an 11.50 kN/m^3 dry unit weight and contains 41% of hygroscopic moisture.

In Table 2, the results of the chemical composition of the soil sample using XFR are shown. Mainly SiO_2, Al_2O_3, and Fe_2O_3 were found, which are usually detected in sedimentary soils and actively participate in the chemical stabilization process of the soils of the Guabirotuba Formation due to silica and alumina.

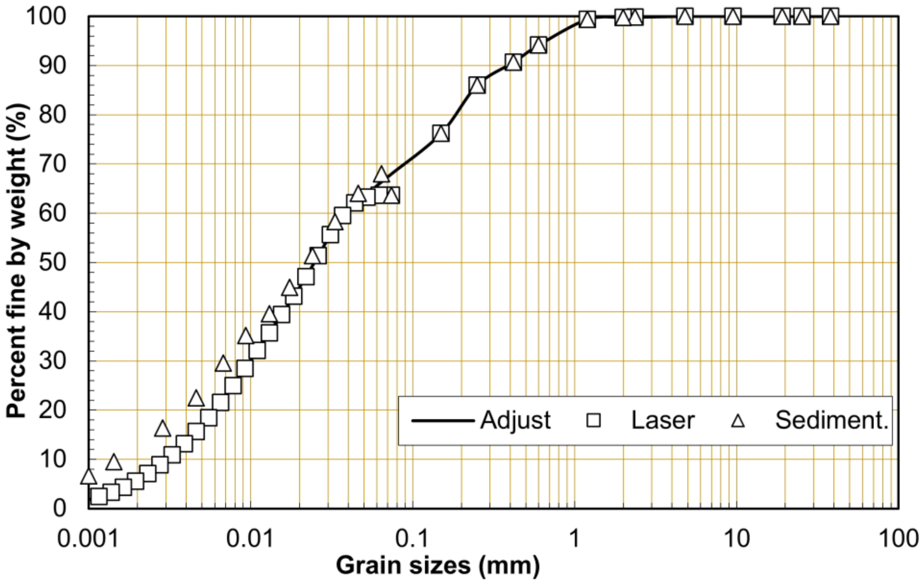

Figure 2. Particle size distribution curve of soil sample

Table 1. Physical properties of the soil

Property	Value
Liquid limit	50.37%
Plastic limit	35.96%
Plastic index	14.41%
Specific gravity of soil	2.63
Medium sand (0.2 < Diameter < 0.6 mm)	8.2%
Fine sand (0.06 < Diameter < 0.2 mm)	22.4%
Silt (0.002 < Diameter < 0.06 mm)	56.5%
Clay (Diameter ≤ 0.002)	7.1%
Mean diameter (D_{50})	0.025 mm
Maximum diameter, D_{max}	0.72 mm
Uniformity coefficient (C_u)	12.88
Curvature coefficient (C_c)	0.88
Color	Yellow

Table 2. Soil and hydrated lime chemical composition by weight

Compost	Concentration by weight (%)	
	Soil	Hydrated lime
SiO_2	48.78	0.70
Al_2O_3	44.51	0.40
Fe_2O_3	0.61	0.20
K_2O	0.84	0.30
TiO_2	0.92	0.20
SO_3	4.12	-
CaO	-	63.2
Na_2O	-	0.10
MgO		10.40
Loss on Ignition (LOI)	0.22	24.50

Hydrated lime was obtained from a local distributor in Curitiba (Paraná) in 20 kg packages, stored in the Geotechnical Laboratory securely, and sealed after each use. Due to the saturation of portlandite in the lime, the pH obtained was 12.4. Lime Fineness was calculated by measuring the number of particles passing through the 200-sieve. Approximately 91% of lime particles are smaller than 0.075 mm in diameter. Table 2 shows the chemical composition of hydrated lime. Calcium oxide is the most significant portion, with 63% by weight, followed by magnesium and silicon oxides, with 10 and 0.7%. Furthermore, it was seen that lime has a high mass loss on fire (24.5%).

Table 3 presents the physical properties of lime. The specific mass of the lime grains was obtained according to NBR 16605 [27], specific for powdered materials. To prevent unintended reactions and reduce the number of variables, all soil and soil–lime mixture characterization tests and test specimens were conducted with distilled water at 23.3°C.

Table 3. Physical properties of the lime

Property	Value
Specific gravity of lime	2.34
pH of saturated solution (25° C)	12.45
$Mg(OH)_2$	0.60%
Maximum diameter (D_{max})	0.004 mm
Diameter < 0.002 mm	91%
Color	White

2.2. Methods

2.2.1. Compaction Test

In accordance with NBR 7182 [28], standard, intermediate, and modified compaction efforts were utilized in soil compaction tests conducted under ASTM D698-12 [29]. To define the molding points, the optimal moisture content and maximum dry unit weight points were extracted from each compaction curve and established for each effort and lime content according to Table 4. The addition of lime reduced unit weight and enhanced optimal water content. The relationship between tensile and compressive strengths as a function of time was subsequently assessed for each of the four curing times: 30, 60, 90, and 180 days.

Table 4. Lime-soil compaction results and molding points

Lime content (%)	Effort	Optimal water content (%)	Maximum dry unit weight (kN/m^3)	Degree of saturation (%)
3%	Standard	24.80	14.15	79.82
	Intermediate	19.00	15.52	75.97
	Modified	16.60	16.41	77.05
5%	Standard	24.80	14.00	77.82
	Intermediate	16.80	15.31	65.09
	Modified	14.30	16.51	67.61
7%	Standard	26.50	13.65	79.03
	Intermediate	19.50	15.16	73.94
	Modified	17.00	16.30	77.81
9%	Standard	27.50	13.67	82.44
	Intermediate	21.00	15.05	78.42
	Modified	19.00	15.99	82.80

2.2.2. Lime Content, Molding, and Curing of Specimens

The pH measurements were taken using a pH meter with a 0 to 14 pH measurement range and an accuracy of 0.015 pH at temperatures ranging from 0 to 100°C. To calibrate the equipment, buffers with pH=7 and pH=10 were used [30]. When 3 percent lime is added, the pH level of the mixture remains constant (Figure 3). To stabilize the silty soil, the following four contents were selected: 3%, 5%, 7%, and 9% of the dry mass of the soil. The pH method has some limitations for use in tropical and subtropical soils. A report by TRB [31] demonstrated that the percentage of lime obtained by the pH method does not produce the maximum compressive strength in tropical and subtropical soils. According to the author, the method does not guarantee whether the reaction of the soil with the lime will produce a substantial increase in strength and should only be used as a reference. Because the soil studied does not belong to the "tropical" classification, this effect is not shown.

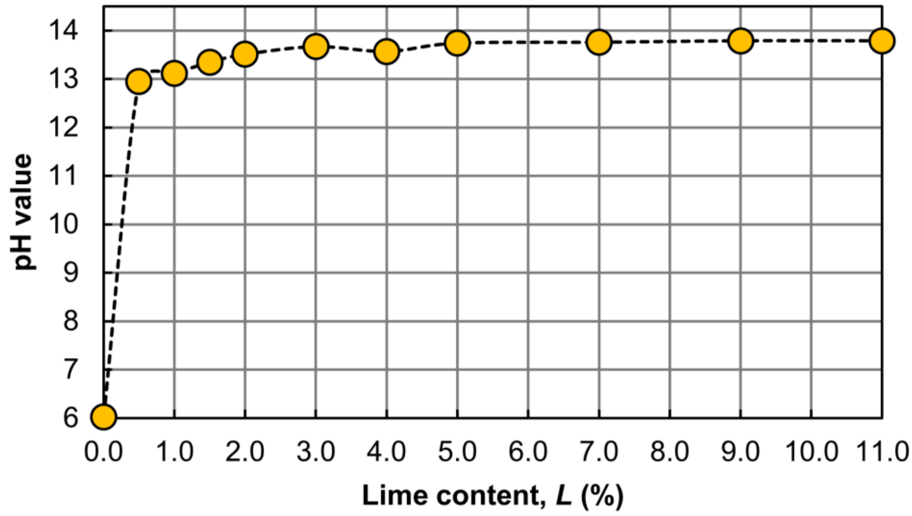

Figure 3. Results of pH test (fixing lime content)

The mixing and molding specimens (for unconfined compressive and split tensile tests-see Figure 4) procedure begins with weighing the materials on a scale with two digits of precision, with subsequent individual packaging of these in plastic bags to preserve their dry conditions. After that, the soil and lime were mixed until they reached uniformity/homogeneity. Subsequently, water was added, and mixing continued for about 10 minutes until a uniform consistency was achieved. The wet and homogenized mixture removed enough material to fill two capsules to check the molding moisture. Subsequently, the mixture was divided into three equal fractions corresponding to the number of layers required for the type of specimen used. The molding was done statically with a hydraulic press in metallic molds. After the static compaction of each layer, the top was scarified in order to guarantee adhesion with the subsequent layer. At the end of molding each specimen, the dimensions (height and diameter) were checked with the caliper and the total mass to calculate the desired optimum compaction parameters in concordance with Figure 5. Then, the specimen was properly sealed in three plastic bags and cured in a closed environment. After compaction and extraction of the specimen, it was identified and packed in plastic packaging and a humid chamber to avoid losing its moisture content during the curing process. The storage temperature was maintained at 23±2°C and a relative humidity of not less than 95%. The specimens with different lime contents were left in the curing process of 30, 60, 90, and 180 days to measure the difference in resistance of the improved soil for each curing period. Regarding molding specifications, a variation of ±1.5% was tolerated in the average dimensions of each specimen, ±1% in its mass, and 5% concerning the average relative humidity (not absolute) measured by the three capsules [32, 33]. If any of these restrictions were not satisfied, the specimen was discarded, and a new one was molded.

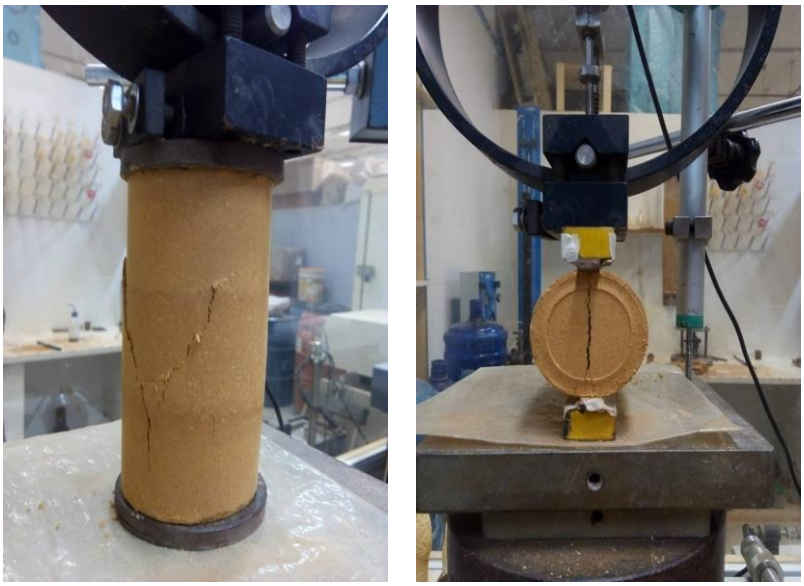

(a) (b)

Figure 4. Unconfined compressive strength (a) Split tensile strength

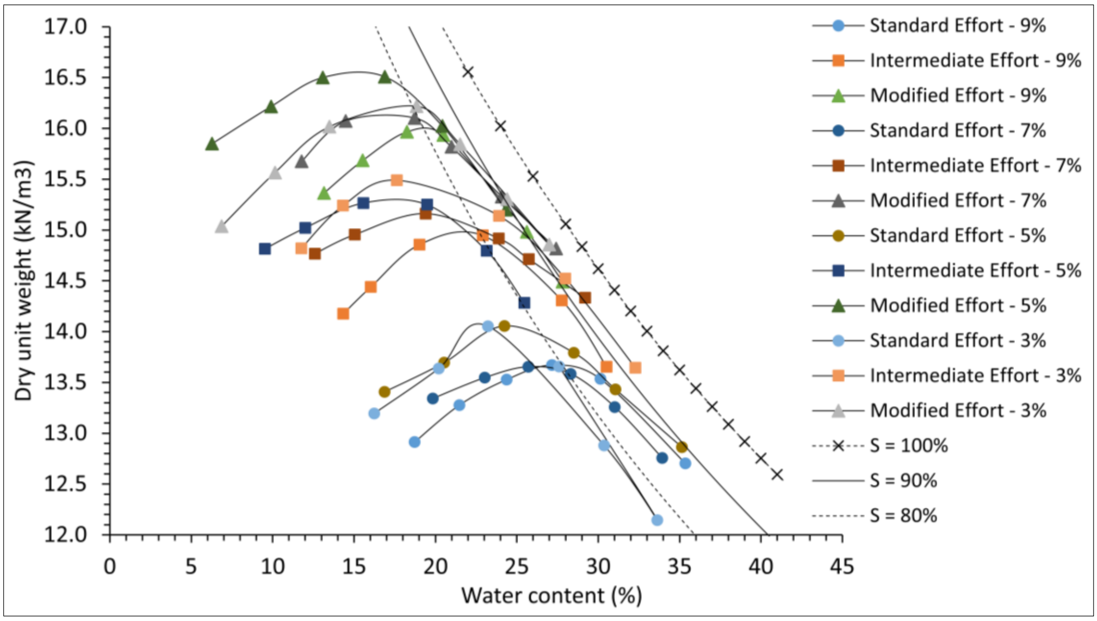

Figure 5. Compaction curves of lime-soil compacted blends

After curing and before rupture, the specimens were immersed for 4 hours. Immediately before testing, they were removed from immersion and superficially dried with absorbent paper. For the rupture of the specimens, an electric press from the Wille Geotecnik brand with a capacity of 100 kN and a test speed of 1 mm/min was used. The test was instrumented with a load cell with a capacity of 50 kN, which performs the applied force readings. No transducer was used to measure the internal displacement; only an external LVDT displacement transducer was employed. A data acquisition unit was utilized to acquire data from the load cell and displacement transducer, and the results were processed by software.

2.2.3. Split Tensile Strength and Unconfined Compressive Strength

The procedures of NBR 5739 [15] were followed for the unconfined compressive strength tests, performed in triplicate cylindrical specimens 10 cm in height and 5 cm in diameter. Unconfined compressive strength tests (q_u) and splitting tensile strength were performed in an automatic press with controlled displacement. A constant displacement rate (1.00 mm/min) was used to measure the mechanical performance of specimens submerged in water for 4 hours; this immersion, one day before the pre-established curing time, aims to saturate the samples and minimize suction effects. The tensile strength tests by diametral compression followed the Brazilian standard NBR 7222 [34]. The split tensile differs only from the unconfined compressive in the positioning of the specimen in the press. This must be such that the axial plane of the specimen, defined by the opposed generatrix, coincides with the load application axis.

2.2.4. Porosity-to-Lime Index

Consoli et al. [35] found a way to reconcile the rates of change of the quantities of volumetric lime content and porosity by applying power over one of them. After several attempts, it was found that applying a power equal to 0.12 on the volumetric binder content parameter would have a better compatibility between the variation rates, resulting in a better fit for the voids/lime ratio. Typically, the behavior of lime-stabilized soils can be evaluated by the ratio of the porosity to the volumetric lime content (η/L_{iv}), where L_{iv} is defined as the ratio of lime volume to the total volume of the specimen and is calculated as follows [36]:

$$\eta=100-\frac{100}{Vs}\left\{\left[\frac{V_s\,\gamma_d}{1+L/100}\left(\frac{S_s}{100}\right)\right]/\gamma_s+\left[\frac{V_s\,\gamma_d}{1+L/100}\left(\frac{L}{100}\right)\right]/\gamma_L\right\} \tag{1}$$

where V_s is the total volume of the specimen; L is the amount of lime about dry soil; γ_d is the dry unit weight of the specimen; S_s is the soil content; and γ_s and γ_L are the specific weights of soil and lime grains, respectively.

3. Results and Discussions

3.1. Effects of Porosity on Split Tensile and Compressive Strengths

Soils treated with lime exhibit a complex mechanical behavior influenced by several factors, among which the amount of added lime, the porosity of the mixture, moisture content, and, mainly, curing time and temperature stand out. Consoli et al. [37], when studying mixtures of a silty-lime soil, observed the influence of the amount of lime and the porosity on the initial stiffness for different curing times studied, verifying that the initial stiffness increases linearly with the increase of the amount of lime and exponentially with the reduction of porosity.

As shown in Figures 6 and 7, the addition of lime results in a dramatic increase in strength as porosity decreases. Authors such as Consoli et al. [38] and Metcalf et al. [19] reported the effect of porosity on strength, concluding that its decrease increased q_u and q_t for various soil types and cementitious agents such as lime, fly-ash, and cement. Figures 6 and 7 show that the strength decreases as the amount of hydrated lime increases. Consequently, the angular coefficients of the strength lines (with varying porosity) increase with curing time for each lime content. Consequently, this phenomenon is most apparent at *L*=9 percent, followed by *L*=7 percent, and then *L*=5 percent. This is because the lime content has increased. Lime contains pozzolanic or cementitious material, increasing the amount of L in the soil and forming a rigid matrix that increases mechanical resistance and decreases porosity.

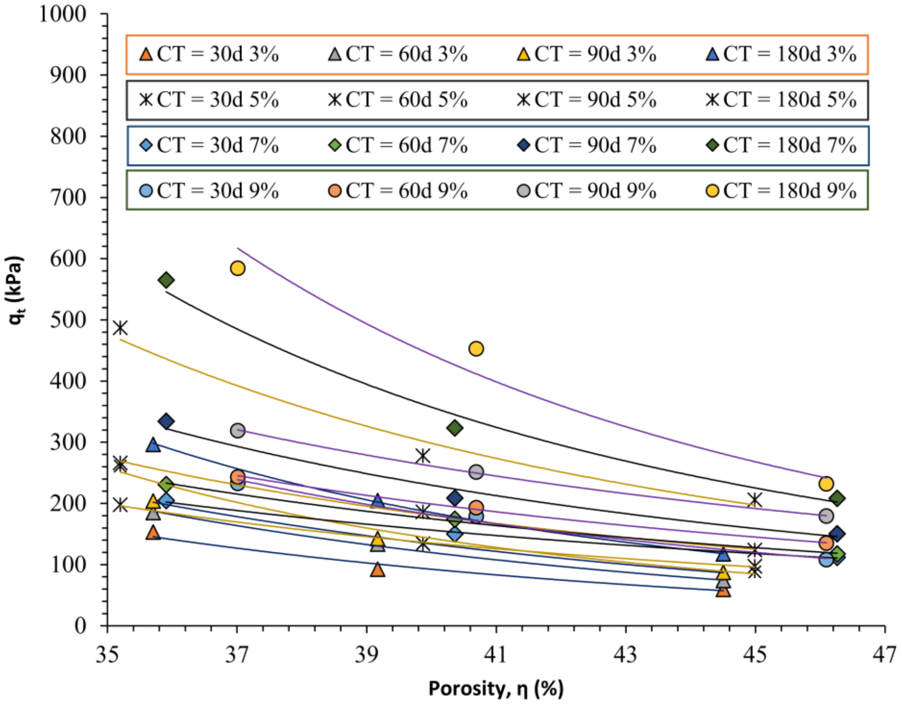

Figure 6. Variation of split tensile strength with porosity

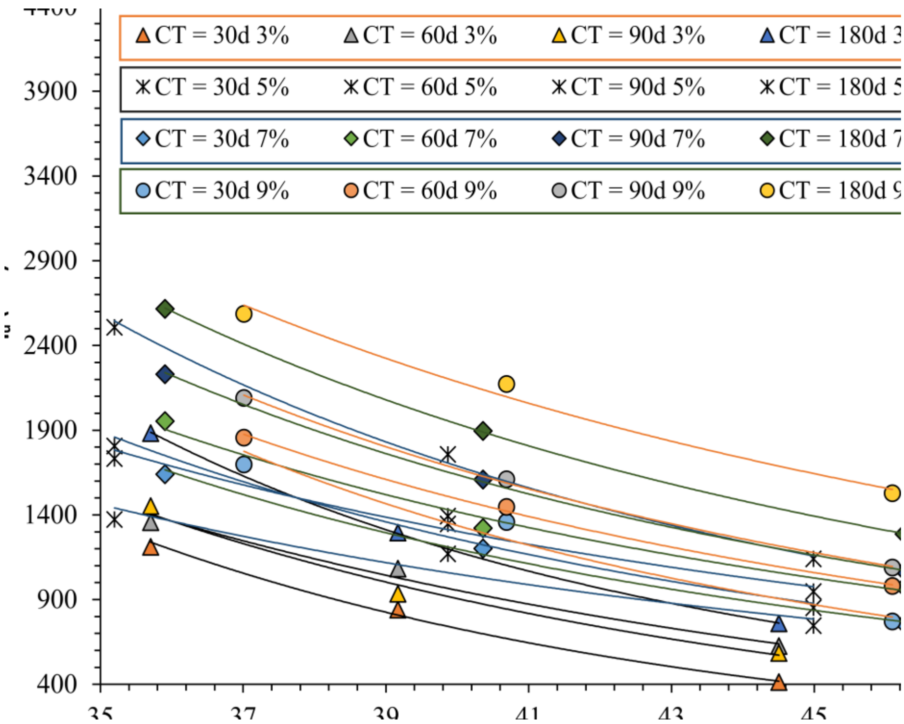

Figure 7. Variation of unconfined compressive strength with porosity

When added to soil, lime reacts with the clay particles and causes them to bind together, reducing porosity. The reduction in porosity leads to an increase in the soil's unconfined compressive and split tensile strength. However, if too much lime is added, the soil can become too brittle and exhibit a decrease in strength. Therefore, finding the optimal lime content for a given soil type is essential to achieve the desired strength and stability. Overall, the porosity/ index can be used to guide the selection of appropriate lime content to achieve the desired strength while avoiding over-stabilization [13]. The optimal porosity/binder index for lime-stabilized soils in the present study depends on the specific application and engineering requirements, such as the desired strength and stability of the soil. For a 1200 kPa of unconfined compressive, 5% of lime is an appropriate stabilizer content [39].

Increasing the amount of lime significantly increased the measured values of compression and traction. In the range of contents studied (3%, 5%, and 7%), the mechanical strength increases non-linearly with the lime percentages. The rate of increase in mechanical strength, represented by the slope of the adjustment lines, did not vary considerably with the increase in the dry apparent specific weight of the compacted material. However, the reduction in the porosity of the compacted material promoted substantial increases in unconfined compression. It was verified that the mechanical resistance potentially increased with the reduction of the porosity of the compacted mixture, an effect observed in all studied curing times (30, 60, 90, and 180 days).

3.2. Effects of Voids/Lime Ratio on Tensile and Compressive Strengths

Figure 8 correlates the unconfined compressive strength results to the porosity index/binder volumetric content ($\eta/L_{iv}^{0.19}$). To reconcile the effects between porosity and binder content, an internal exponent of 0.19 was established, a value previously used by studies that stabilized silty and clayey soils [33, 40]. Figure 8 shows lower porosity and higher binder content (i.e., lower $\eta/L_{iv}^{0.19}$ value) resulted in higher unconfined compressive strength. Lower porosity, achieved through more excellent compaction, increases the contact area between soil and binder particles, leading to more outstanding interlocking and significant friction mobilization. The increase in the binder content results in more significant precipitation of cementitious compounds and an increase in strength. In both binders, there was a significant increase in unconfined compressive strength due to increased curing time and amount of lime, especially for the last factor. Notably, the lime content showed an average strength gain of 75% after 60 days of curing compared to the resistance after 30 days of curing. This value is compatible with the 30-day resistance gain of initial high-strength cement mortars, which can vary between 70-90% of the resistance gain after 28 days of curing. In addition, high coefficients of determination (R^2) were found between unconfined compressive strength and the $\eta/L_{iv}^{0.19}$ index, which indicates the viability of the index in predicting q_u.

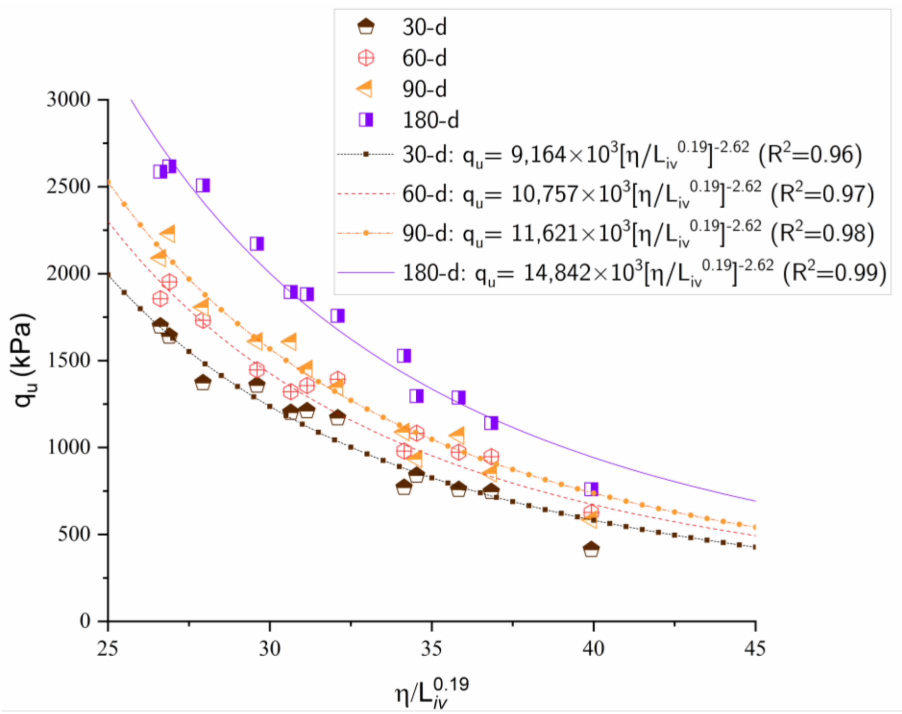

Figure 8. Variation of unconfined compressive strength with η/Liv0.19 ratio for 30, 60, 90, and 180 days of curing

Figure 9 relates the results of split tensile strength to the porosity index/binder volumetric content ($\eta/L_{iv}^{0.19}$). It is observed in Figure 9 that a lower value of $\eta/L_{iv}^{0.19}$ caused an increase in the split tensile strength. As analysed in the unconfined compressive strength, more excellent compaction (i.e., reduced porosity) increases the contact area between soil and binder particles, resulting in more significant friction mobilization. Furthermore, the increase in the binder content leads to more significant precipitation of cementitious compounds and an increase in strength. In both binders, there is a significant increase in split tensile strength due to higher curing time.

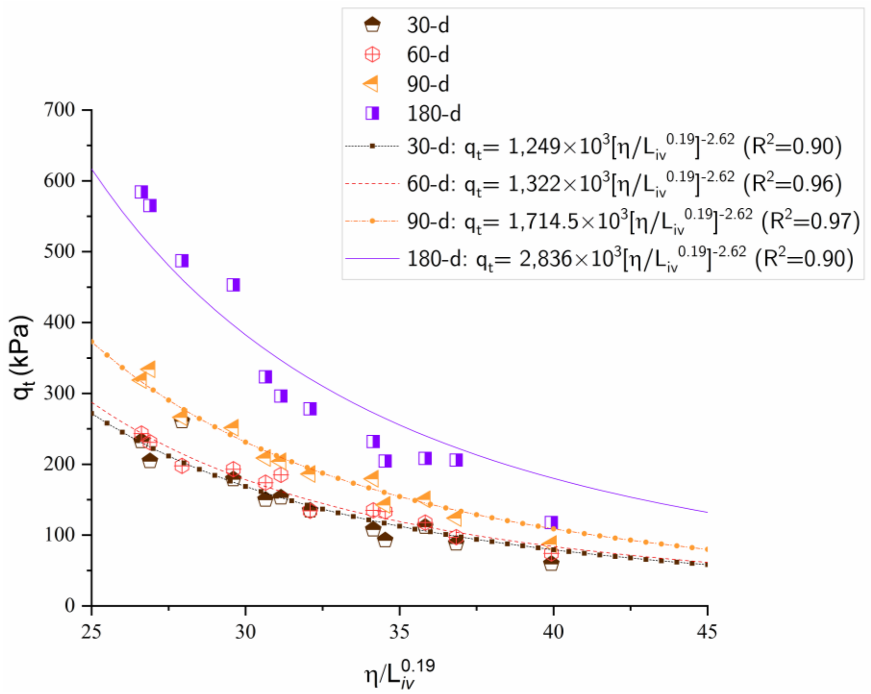

Figure 9. Variation of split tensile strength with η/Liv0.19 ratio for 30, 60, 90, and 180 days of curing

This effect on tensile strength is direct and is proportional to the compaction effort required to meet the dry unit weight of molding and the volume of each mixture material: soil and lime of η/L_{iv}-q_u and η/L_{iv}-q_t was best represented by a potential equation optimized with the parameters x (=0.19) and B (=2.20) obtained from Table 5 for each lime percentage and mechanical resistance of splitting tensile and compressive. This indicates that the inverse of L_{iv} $(1/L_{iv})$ is directly proportional to the values of q_u and qt, but an adjustment to the value x is required to compensate for the percentage of voids in each specimen and make it mathematically proportional to the porosity. According to recent research by Rios et al. [41], the values of q_u and q_t are equally dependent on another adjusted and optimized value k, which depends on the soil type (granulometry, mineralogy, plasticity limits) and the type of binder used. The value of negative B (-B) denotes an inverse potential equation in which the relations $\eta/{L_{iv}}^{x}$-q_u and $\eta/{L_{iv}}^{x}$-q_t t increase with the reduction of voids and the addition of lime [42, 43]. These results are independent of the compaction curves shown in Figure 5 (and summarized in Table 5) of the mixtures, where adding lime decreased the soil density and increased the amount of water due to the property of absorption of lime.

Table 5. Equations controlling splitting tensile/compressive strength ratio to distinct curing times

Curing time	Equations for q_t/q_u ratio
30	$\xi=\frac{q_t}{q_u}=\frac{1{,}249\times10^3\left[\frac{\eta}{(L_{iv})^{0.19}}\right]^{-2.62}}{9{,}164\times10^3\left[\frac{\eta}{(L_{iv})^{0.19}}\right]^{-2.62}}=0.136$
60	$\xi=\frac{q_t}{q_u}=\frac{1{,}322\times10^3\left[\frac{\eta}{(L_{iv})^{0.19}}\right]^{-2.62}}{10{,}757\times10^3\left[\frac{\eta}{(L_{iv})^{0.19}}\right]^{-2.62}}=0.129$
90	$\xi=\frac{q_t}{q_u}=\frac{1{,}714.5\times10^3\left[\frac{\eta}{(L_{iv})^{0.19}}\right]^{-2.62}}{11{,}621\times10^3\left[\frac{\eta}{(L_{iv})^{0.19}}\right]^{-2.62}}=0.147$
180	$\xi=\frac{q_t}{q_u}=\frac{2{,}836\times10^3\left[\frac{\eta}{(L_{iv})^{0.19}}\right]^{-2.62}}{14{,}842\times10^3\left[\frac{\eta}{(L_{iv})^{0.19}}\right]^{-2.62}}=0.190$

A lower porosity/binder index indicates a higher level of stabilization, which leads to a denser microstructure with fewer voids and interstitial spaces between particles. The denser microstructure of the soil reduces the permeability or the ease with which water can flow through the soil. It also increases the soil's load-bearing capacity making it more suitable for construction applications that require a stable foundation [44]. Conversely, a higher porosity/binder index indicates a lower level of stabilization, which leads to a less dense microstructure with more voids and interstitial spaces. The less-dense microstructure of the soil results in lower load-bearing capacity and increased permeability. This may be desirable for specific applications, such as soil that is used for drainage or landscaping. Therefore, the porosity/binder index plays a critical role in determining the microstructure of stabilized soils and can be used to optimize soil performance in a wide range of applications. A careful selection of the porosity/binder index can result in stabilized soil with the desired properties, such as high strength, low permeability, and increased stability, while ensuring that the soil retains the required porosity level for specific applications [2, 4].

Lime-soil is a chemical reaction when lime is mixed with fine-grained soils. These reactions can be classified into two relatively well-defined stages: a rapid process (minutes to days, sometimes months) in which there is an improvement in the plasticity of the material, but little permanent strength is developed, and a slow process (weeks to years) of resistance development, with the formation of cementing products. Reactions require water to start. The first event is the dissociation of the calcium hydroxide molecule. Reactions capable of increasing resistance are those that proceed slowly and are called pozzolanic reactions. Pozzolanic reactions occur with materials containing silica and alumina, which react with lime when finely divided in the presence of water. For pozzolanic reactions to occur, silica and alumina must be solubilized. The reaction products of high CaO systems resemble those originating from cement hydration, mainly the C-A-S-H gel (Ca/Si between 1 and 1.2) and secondary mineral products such as hydrotalcite, calcite and calcite AFm (calcium monosulfoaluminate). It is also possible to form a C-(N)-A-S-H gel due to the replacement of Ca+2 in the polymers by Na+.

3.3. Split Tensile-to-Compressive Strength Ratio

Since the increase in tensile strength is proportional to simple compression, a direct relationship between the two can be established. Thus, Figure 10 presents the relationship between the simple compression and the diametric traction of the soil-cement samples. It can be noticed that the ratio is 0.15, with variations of 0.20 (on top) and 0.12 (on the bottom). Consoli et al. [45], when studying mixtures of Osório sand with Portland cement whose cement contents were 1, 2, 3, 5, 7, 9, and 12% in specimens with three different dry specific weights, found that the ratio between the tensile strength by diametral compression and simple compression was equal to 0.15, regardless of the porosity index/volumetric cement content. Consequently, dosage methodologies based on rational criteria can focus, for this material, both on tensile and simple compression tests, being able to obtain the result of one from the result of the other since they are interdependent. In addition, Consoli et al. [37], using the same voids/lime concept, treated a sandy silt soil mixed with different proportions of ash (12.5%, 25%, and 50%) with 3%, 5%, 7%, and 9% lime. Unconfined compression tests were carried out for each percentage of lime, molded to different apparent dry masses, and cured for different curing times. The voids/lime ratio, expressed in the form of porosity/volumetric lime content, with the results of simple compression of soil-lime samples with 25% fly ash previously cured for 28, 60, and 90 days. To make the magnitudes compatible, the author used a power equal to 0.12, which did not vary with the curing time. The split tensile-compressive index was calculated as 0.12.

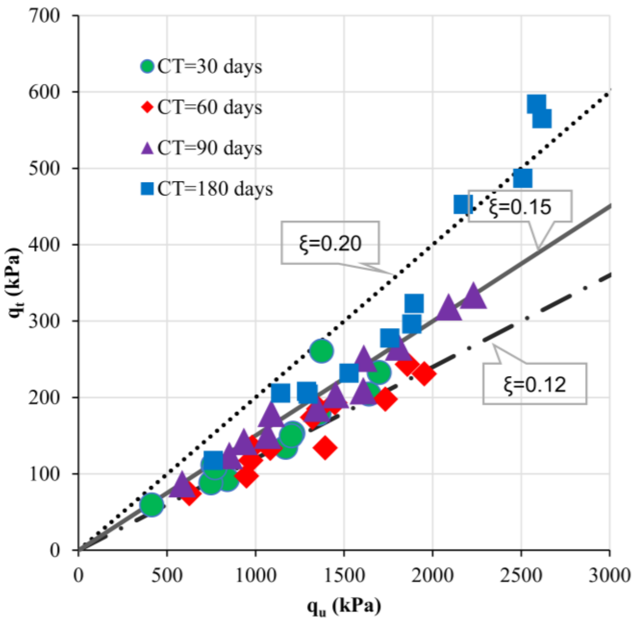

Figure 10. Direct relationship of split tensile/compression strength ratio

According to Schnaid et al. [46], there is a general understanding that, for a given stress variation, the shear strength of naturally and artificially cemented soils can be constituted by a straight rupture envelope of Mohr-Coulomb, delineated by a cohesive intercept, which is only a function of cementation, and by a natural internal friction angle between particles, which somehow does not seem to be affected by cementation. For Coop and Atkinson [47], during the shearing of cemented soils, there are three ways of behavior to be observed, and these depend on the initial state of the specimen concerning the plasticization curve of the cementitious connections. At low confining stresses, when the cementation remains intact, i.e., the resistance of the cementitious connections is more excellent than the confining stress, the soil behavior is elastic up to a certain well-defined plastification point and outside the boundary surface for uncemented soils, accompanied by a sharp drop in resistance towards the critical state (curve C), exhibiting a fragile and dilating behavior. At intermediate confining stresses, even if the cementitious connections remain intact at the beginning of the test, plastification occurs during shearing, with fundamentally frictional rupture (curve B). A defined plasticization point can occur after an initial elastic behavior without a prominent resistance peak in this intermediate state. However, the behavior is ductile and compressive at high confining stresses since the cementation between particles is broken during isotropic compression (curve A), a defined plasticizing point, and peak resistance. After all, all three curves (A, B, and C) converge, for large strains, on the critical state line.

Finally, the tensile-compressive ratio provides a handy parameter because it allows estimating the values of q_t or q_u starting from a single real value between them. Therefore, the empirical mechanical compressive strengths and splitting can also be established tensile quickly in the field.

3.4. Effects of Curing Time on Split Tensile and Unconfined Compressive

As proposed by Baldovino et al. [48], a constant is obtained by dividing each empirical equation for q_t and q_u (shown in Figures 6 and 7, respectively) by the expression $10^3(\eta/L_{iv}^{0.19})^{-2.62}$, which increases with the curing time (CT). Figure 11 depicts the evolution of the split tensile and compressive strength from 30 to 180 days of curing. Each obtained constant is correlated to its respective curing time. Increasing the curing time causes qt and q_u to increase linearly, with R^2 for q_u equal 0.99 and R^2 for qt equal 0.98. Regarding the $\eta/L_{iv}^{0.19}$ ratio and curing time, a dosage equation for qt and q_u can be proposed (CT).

The dosage equations for unconfined compressive and split tensile are:

$$q_u = [37.19CT + 8204] \times 10^3[\eta/L_{iv}^{0.19}]^{-2.62} \tag{2}$$

$$q_t = [11.16CT + 776] \times 10^3[\eta/L_{iv}^{0.19}]^{-2.62} \tag{3}$$

Equations 2 and 3 demonstrate a linear tendency for the increase in the normalized resistance of the soil-lime mixtures with the increase in the curing time. This normalization is possible to carry out using the porosity/cal factor. Thus, it can be concluded that it is the main factor that affects the resistance of the mixes at any curing time, compaction energy, and the amount of lime used.

According to Consoli et al. [49], these percentages indicate that suction had almost no effect on the strength results, so it is not considered a relevant and analysable variable in the research. The optimal application of the dosage equations [Equations 2 and 3] in civil construction projects (slopes/road pavements/rammed earth/foundations) depends not only on the compaction equipment to be used on the field but also on the soil volume, as adding 9 percent lime content may render the project economically unviable. Due to their minimum q_u=1200 kPa, options with low lime contents of 5 percent and modified effort would be suitable for subbase applications. In any case, builders have various options depending on the project's needs.

Metcalf et al. [19] presented a study on the influence of the curing time in different types of soils treated with 5% hydrated lime, observing the rates of more significant strength gains in sands. Cementing agents of pozzolanic nature, artificially introduced in soil stabilization mechanisms, have to cure time as one of the most significant variables for characterizing the mechanical behavior since this factor directly affects the effectiveness of the degree of cementation of the mixture. Soils treated with lime exhibit a complex mechanical behavior influenced by several factors, among which the amount of lime added, the porosity of the mixture, the moisture content, and the curing time stand out.

The structural support of lime-stabilized soils can be utilized in pavement design. Lime can be used in the treatment of soils in the Guabirotuba Formation, in various degrees or amounts, depending on the objective and the porosity/lime ratio. A minimum amount of 5% lime for treatment can be used to dry and modify the local soils of Curitiba-Brazil temporarily. Mixture design equations are based on the porosity/lime ratio and the normalization of the increase in resistance as a function of curing time (Figure 11). Typically, 1-4% lime by weight of soil is employed for amendment, which is generally less than that used for permanent soil stabilization. However, due to the soil properties used in this study, it is recommended to use 5%.

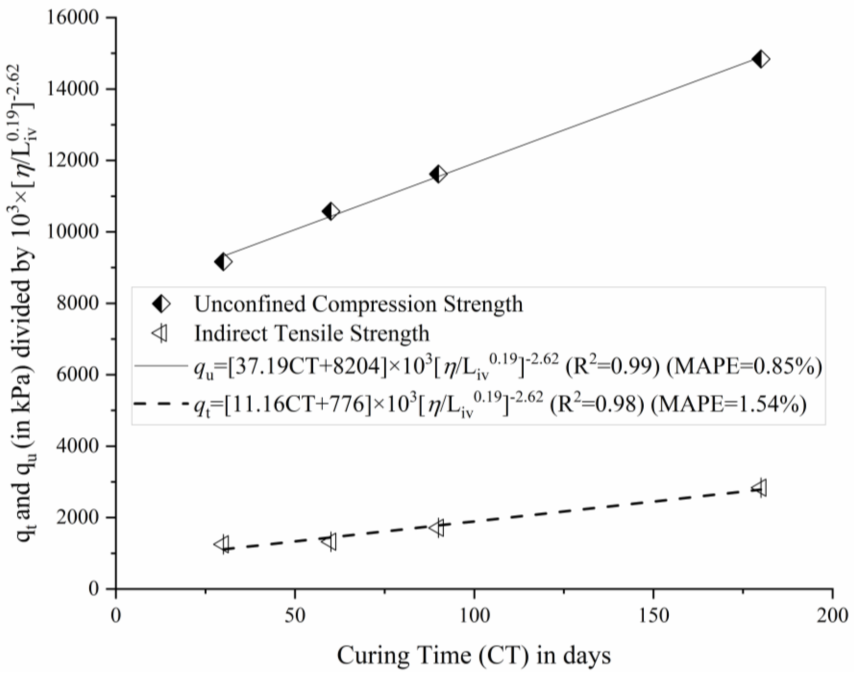

Figure 11. Variation of unconfined compressive strength (q_u) and split tensile strength (q_t) with curing time (CT)

4. Conclusions

Based on the experimental and theoretical data presented in this research and taking into account the limitations of the study, the following conclusions can be drawn:

- This study developed equations for estimating the unconfined compressive strength and split tensile strength of lime-stabilized yellow soil from the Guabirotuba geological formation in Curitiba, Brazil. As depicted in Figure 11, the equations were validated by approximating the experimental values with a 98 percent adjustment and a close to one percent error. It is a single potential trend of q_u and q_t as a function of curing periods and apparent dry unit weights. This single trend can be applied to all molding conditions of the silty soils stabilized in this study with hydrated lime and pozzolanic cement.
- The porosity/volumetric lime content ratio ($\eta/L_{iv}^{0.19}$) can be set as a parameter that influences and estimates the strength of the optimally compacted, lime-stabilized soil studied in this paper. After several days of curing, initial molding porosity and lime quantity decreased in tensile and unconfined compression strength for all soil-lime mixtures studied. These findings conclude that the porosity/lime ratio controls the resistance on the stabilized soil in optimal compaction conditions. A result that had not been explored before. Nevertheless, the results are limited to the percentages of calves used from 3% to 9%, without implying increasing or decreasing compaction energy.
- It is possible to obtain the same splitting tensile and unconfined compressive strength through various lime-soil mixture combinations. The contents depend on the project specifications, compaction energy, and construction economics.
- An index of $0.15=q_t/q_u$ was determined for the lime-soil mixtures. Lime content and porosity/lime index do not impact the q_t/q_u ratio as a cement-soil stabilization process. According to previous soil stabilization studies in Guabirotuba, values between 0.15 and 0.20 correspond.
- Energy-compacted mixtures are recommended for geotechnical engineering projects. Even though intermediate energy meets the standard's requirements (greater than 5 percent lime), it is not recommended for use because it requires heavy compaction in many situations, such as for heavy haul railway, the base of pavements, and the impervious core of earth dams.

5. Declarations

5.1. Author Contributions

Conceptualization, W.T.; methodology, W.T.; formal analysis, J.A.B.; writing—review and editing, W.T., R.I., and J.A.B.; supervision, R.I. All authors have read and agreed to the published version of the manuscript.

5.2. Data Availability Statement

The data presented in this study are available in the article.

5.3. Funding

Finance Code 001 of the Coordenacão de Aperfeiçoamento de Pessoal de Nivel Superior - Brasil (CAPES) partially funded this study. The authors thank the Conselho Nacional de Desenvolvimento Científico e Tecnológico (CNPq) and Fundação Araucária do Paraná.

5.4. Conflicts of Interest

The authors declare no conflict of interest.

6. References

[1] Consoli, N. C., Da Silva Lopes, L., Foppa, D., & Heineck, K. S. (2009). Key parameters dictating strength of lime/cement-treated soils. Proceedings of the Institution of Civil Engineers: Geotechnical Engineering, 162(2), 111–118. doi:10.1680/geng.2009.162.2.111.

[2] Saldanha, R. B., & Consoli, N. C. (2021). Compressibility, Durability and Strength of Coal Fly Ash–Carbide Lime–Sodium Chloride Blends. International Journal of Geosynthetics and Ground Engineering, 7(2). doi:10.1007/s40891-021-00286-7.

[3] Mohammadinia, A., Arulrajah, A., D'Amico, A., & Horpibulsuk, S. (2018). Alkali-activation of fly ash and cement kiln dust mixtures for stabilization of demolition aggregates. Construction and Building Materials, 186, 71–78. doi:10.1016/j.conbuildmat.2018.07.103.

[4] Arulrajah, A., Mohammadinia, A., D'Amico, A., & Horpibulsuk, S. (2017). Effect of lime kiln dust as an alternative binder in the stabilization of construction and demolition materials. Construction and Building Materials, 152, 999–1007. doi:10.1016/j.conbuildmat.2017.07.070.

[5] Arulrajah, A., Mohammadinia, A., Phummiphan, I., Horpibulsuk, S., & Samingthong, W. (2016). Stabilization of Recycled Demolition Aggregates by Geopolymers comprising Calcium Carbide Residue, Fly Ash and Slag precursors. Construction and Building Materials, 114, 864–873. doi:10.1016/j.conbuildmat.2016.03.150.

[6] Arulrajah, A., Ali, M. M. Y., Disfani, M. M., & Horpibulsuk, S. (2014). Recycled-Glass Blends in Pavement Base/Subbase Applications: Laboratory and Field Evaluation. Journal of Materials in Civil Engineering, 26(7), 4014025. doi:10.1061/(asce)mt.1943-5533.0000966.

[7] Arulrajah, A., Kua, T. A., Suksiripattanapong, C., & Horpibulsuk, S. (2019). Stiffness and strength properties of spent coffee grounds-recycled glass geopolymers. Road Materials and Pavement Design, 20(3), 623–638. doi:10.1080/14680629.2017.1408483.

[8] Arulrajah, A., Kua, T. A., Suksiripattanapong, C., Horpibulsuk, S., & Shen, J. S. (2017). Compressive strength and microstructural properties of spent coffee grounds-bagasse ash based geopolymers with slag supplements. Journal of Cleaner Production, 162, 1491–1501. doi:10.1016/j.jclepro.2017.06.171.

[9] Hoch, B. Z., Diambra, A., Ibraim, E., Festugato, L., & Consoli, N. C. (2022). Strength and stiffness of compacted chalk putty–cement blends. Acta Geotechnica, 17(7), 2955–2969. doi:10.1007/s11440-021-01415-2.

[10] Rios, S., Viana da Fonseca, A., & Baudet, B. A. (2014). On the shearing behaviour of an artificially cemented soil. Acta Geotechnica, 9(2), 215–226. doi:10.1007/s11440-013-0242-7.

[11] Pereira dos Santos, C., Bruschi, G. J., Mattos, J. R. G., & Consoli, N. C. (2022). Stabilization of gold mining tailings with alkali-activated carbide lime and sugarcane bagasse ash. Transportation Geotechnics, 32. doi:10.1016/j.trgeo.2021.100704.

[12] Baldovino, J. A., Izzo, R., & Ekinci, A. (2022). Strength Relationship Equation for Artificially Stabilized Rammed Sedimentary Soils. Buildings, 12(9). doi:10.3390/buildings12091433.

[13] de Jesús Arrieta Baldovino, J., dos Santos Izzo, R. L., & Ekinci, A. (2023). Strength, durability, and microstructure of lime production residue glass powder binder-based geomaterial. Acta Geotechnica, 18(3), 1593–1606. doi:10.1007/s11440-022-01678-3.

[14] Tiwari, N., Satyam, N., & Puppala, A. J. (2021). Effect of Synthetic Geotextile on Stabilization of Expansive Subgrades: Experimental Study. Journal of Materials in Civil Engineering, 33(10). doi:10.1061/(asce)mt.1943-5533.0003901.

[15] NBR 5739. (2007). Concrete-compression test of cylindrical specimens-method of test. Brazilian National Standards Organization (ABNT), São Paulo, Brazil. (In Portuguese).

[16] Quiñónez Samaniego, R. A., Scheuermann Filho, H. C., de Araújo, M. T., Bruschi, G. J., Festugato, L., & Consoli, N. C. (2023). Key parameters controlling strength and resilient modulus of a stabilised dispersive soil. Road Materials and Pavement Design, 24(1), 279–294. doi:10.1080/14680629.2021.2013937.

[17] Ferreira, F. A., Desir, J. M., Lima, G. E. S. de, Pedroti, L. G., Franco de Carvalho, J. M., Lotero, A., & Consoli, N. C. (2023). Evaluation of mechanical and microstructural properties of eggshell lime/rice husk ash alkali-activated cement. Construction and Building Materials, 364, 129931. doi:10.1016/j.conbuildmat.2022.129931.

[18] Oluremi, J. R., Eberemu, A. O., Ijimdiya, S. T., & Osinubi, K. J. (2019). Lateritic soil treated with waste wood ash as liner in landfill construction. Environmental and Engineering Geoscience, 25(2), 127–139. doi:10.2113/EEG-2023.

[19] Metcalf, D., Warner, N. L., Nossal, G. J. V., Miller, J. F. A. P., Shortman, K., & Rabellino, E. (1975). Growth of B lymphocyte colonies in vitro from mouse lymphoid organs. Nature, 255(5510), 630–632. doi:10.1038/255630a0.

[20] Ordoñez Muñoz, Y., Luis dos Santos Izzo, R., Leindorf de Almeida, J., Arrieta Baldovino, J., & Lundgren Rose, J. (2021). The role of rice husk ash, cement and polypropylene fibers on the mechanical behavior of a soil from Guabirotuba formation. Transportation Geotechnics, 31, 100673. doi:10.1016/j.trgeo.2021.100673.

[21] ASTM D 2487-17. (2020). Standard Practice for Classification of Soils for Engineering Purposes (Unified Soil Classification System), ASTM International, Pennsylvania, United States. doi:10.1520/D2487-17.

[22] ASTM D4318-17e1. (2018). Standard Test Methods for Liquid Limit, Plastic Limit, and Plasticity Index of Soils. ASTM International, Pennsylvania, United States. doi:10.1520/D4318-17E01.

[23] ASTM D854-14. (2016). Standard Test Methods for Specific Gravity of Soil Solids by Water Pycnometer. ASTM International, Pennsylvania, United States. doi:10.1520/D0854-14.

[24] Rogers, C. D. F., Ceng, M., Glendinning, S., & Roff, T. E. J. (1997). Lime modification of clay soils for construction expediency. Proceedings of the Institution of Civil Engineers: Geotechnical Engineering, 125(4), 242–249. doi:10.1680/igeng.1997.29660.

[25] NBR 7181. (2016). Granulometric Analysis. Brazilian National Standards Organization (ABNT), São Paulo, Brazil. (In Portuguese).

[26] DER-SP M 196/89. (1989). Classification of tropical soils according to the MCT methodology. DNER, Department of Roads and Highways, São Paulo, Brazil.

[27] NBR 16605-14. (2017). Portland cement and other powdered materials - Determination of specific mass. Brazilian National Standards Organization (ABNT), São Paulo, Brazil. (In Portuguese).

[28] NBR 7182. (2016). Soil - Compaction Test, Brazilian Association of Technical Standards. Brazilian National Standards Organization (ABNT), São Paulo, Brazil. (In Portuguese).

[29] ASTM D698-12. (2014). Standard test method for laboratory compaction characteristics of soil using standard effort (12 400 ft-ibf/ft^3 (600 kN-mlm^3)). ASTM International, Pennsylvania, United States. doi:10.1520/D0698-12.

[30] Baldovino, J. A., Moreira, E. B., Teixeira, W., Izzo, R. L. S., & Rose, J. L. (2018). Effects of lime addition on geotechnical properties of sedimentary soil in Curitiba, Brazil. Journal of Rock Mechanics and Geotechnical Engineering, 10(1), 188–194. doi:10.1016/j.jrmge.2017.10.001.

[31] Mills, L., Ivey, S., & Golias, M. M. (2010). Effectiveness of Freeway Truck Operation Safety Measures: Review of Current Research. Transportation Research Board 89th Annual Meeting, Transportation Research Board, Washington, United States.

[32] Saldanha, R. B., da Rocha, C. G., Caicedo, A. M. L., & Consoli, N. C. (2021). Technical and environmental performance of eggshell lime for soil stabilization. Construction and Building Materials, 298. doi:10.1016/j.conbuildmat.2021.123648.

[33] Tonini de Araújo, M., Tonatto Ferrazzo, S., Jordi Bruschi, G. J., & Consoli, N. C. (2021). Mechanical and Environmental Performance of Eggshell Lime for Expansive Soils Improvement. Transportation Geotechnics, 31. doi:10.1016/j.trgeo.2021.100681.

[34] NBR 7222. (2011). Concrete and mortar — Determination of tensile strength by diametric compression of cylindrical specimens. Brazilian National Standards Organization (ABNT), São Paulo, Brazil. (In Portuguese).

[35] Consoli, N. C., Foppa, D., Festugato, L., & Heineck, K. S. (2007). Key Parameters for Strength Control of Artificially Cemented Soils. Journal of Geotechnical and Geoenvironmental Engineering, 133(2), 197–205. doi:10.1061/(asce)1090-0241(2007)133:2(197).

[36] Consoli, N. C., Corte, M. B., & Festugato, L. (2012). Key parameter for tensile and compressive strength of fibre-reinforced soil-lime mixtures. Geosynthetics International, 19(5), 409–414. doi:10.1680/gein.12.00026.

[37] Consoli, N. C., Dalla Rosa Johann, A., Gauer, E. A., Dos Santos, V. R., Moretto, R. L., & Corte, M. B. (2012). Key parameters for tensile and compressive strength of silt-lime mixtures. Geotechnique Letters, 2(3), 81–85. doi:10.1680/geolett.12.00014.

[38] Consoli, N. C., Quiñónez, R. A., González, L. E., & López, R. A. (2017). Influence of Molding Moisture Content and Porosity/Cement Index on Stiffness, Strength, and Failure Envelopes of Artificially Cemented Fine-Grained Soils. Journal of Materials in Civil Engineering, 29(5). doi:10.1061/(asce)mt.1943-5533.0001819.

[39] Tex-120-E. (2013). Test procedure for soil-cement testing. Texas Department of Transportation, (TxDOT), Austin, United States.

[40] Baldovino, J. de J. A., Moreira, E. B., Carazzai, É., Rocha, E. V. de G., dos Santos Izzo, R., Mazer, W., & Rose, J. L. (2021). Equations controlling the strength of sedimentary silty soil–cement blends: influence of voids/cement ratio and types of cement. International Journal of Geotechnical Engineering, 15(3), 359–372. doi:10.1080/19386362.2019.1612134.

[41] Rios, S., Viana Da Fonseca, A., Consoli, N. C., Floss, M., & Cristelo, N. (2013). Influence of grain size and mineralogy on the porosity/cement ratio. Geotechnique Letters, 3(3), 130–136. doi:10.1680/geolett.13.00003.

[42] Baldovino, J. de J. A., Izzo, R. L. dos S., Silva, É. R. da, & Rose, J. L. (2021). Closure to "Sustainable Use of Recycled-Glass Powder in Soil Stabilization" by Jair de Jesús Arrieta Baldovino, Ronaldo Luis dos Santos Izzo, Érico Rafael da Silva, and Juliana Lundgren Rose. Journal of Materials in Civil Engineering, 33(4). doi:10.1061/(asce)mt.1943-5533.0003685.

[43] Baldovino, J. de J. A., Izzo, R. L. dos S., Pereira, M. D., Rocha, E. V. de G., Rose, J. L., & Bordignon, V. R. (2021). Closure to "Equations Controlling Tensile and Compressive Strength Ratio of Sedimentary Soil–Cement Mixtures under Optimal Compaction Conditions" by Jair de Jesús Arrieta Baldovino, Ronaldo Luis dos Santos Izzo, Mirian Dayane Pereira, Eduardo Vieira de Goes Rocha, Juliana Lundgren Rose, and Vitor Reinaldo Bordignon. Journal of Materials in Civil Engineering, 33(4), 7021002. doi:10.1061/(asce)mt.1943-5533.0003671.

[44] Scheuermann Filho, H. C., Beck Saldanha, R., Gravina da Rocha, C., & Cesar Consoli, N. (2021). Sustainable Binders Stabilizing Dispersive Clay. Journal of Materials in Civil Engineering, 33(3). doi:10.1061/(asce)mt.1943-5533.0003595.

[45] Consoli, N. C., Cruz, R. C., Floss, M. F., & Festugato, L. (2010). Parameters Controlling Tensile and Compressive Strength of Artificially Cemented Sand. Journal of Geotechnical and Geoenvironmental Engineering, 136(5), 759–763. doi:10.1061/(asce)gt.1943-5606.0000278.

[46] Schnaid, F., Prietto, P. D. M., & Consoli, N. C. (2001). Characterization of Cemented Sand in Triaxial Compression. Journal of Geotechnical and Geoenvironmental Engineering, 127(10), 857–868. doi:10.1061/(asce)1090-0241(2001)127:10(857).

[47] Coop, M. R., & Atkinson, J. H. (1994). The mechanics of cemented carbonate sands. Geotechnique, 44(3), 533–537. doi:10.1680/geot.1994.44.3.533.

[48] Baldovino, J. A., Moreira, E. B., Izzo, R. L. dos S., & Rose, J. L. (2018). Empirical Relationships with Unconfined Compressive Strength and Split Tensile Strength for the Long Term of a Lime-Treated Silty Soil. Journal of Materials in Civil Engineering, 30(8), 6018008. doi:10.1061/(asce)mt.1943-5533.0002378.

[49] Consoli, N. C., Festugato, L., Da Rocha, C. G., & Cruz, R. C. (2013). Key parameters for strength control of rammed sand-cement mixtures: Influence of types of portland cement. Construction and Building Materials, 49, 591–597. doi:10.1016/j.conbuildmat.2013.08.062.